

# Regression-based Age Prediction of Plastic Waste using Hyperspectral Imaging

Felix Kronenwett<sup>1</sup>, Pia Klingenberg<sup>2</sup>, Georg Maier<sup>1</sup>, Thomas Längle<sup>1</sup>,  
Elke Metzsch-Zilligen<sup>2</sup>, and Jürgen Beyerer<sup>1,3</sup>

<sup>1</sup> Fraunhofer Institute of Optronics, System Technologies and Image Exploitation IOSB, Fraunhoferstraße 1, 76131 Karlsruhe, Germany

<sup>2</sup> Fraunhofer Institute for Structural Durability and System Reliability LBF, Bartningstraße 47, 64289 Darmstadt, Germany

<sup>3</sup> Vision and Fusion Laboratory (IES), Karlsruhe Institute of Technology (KIT), Haid-und-Neu-Str. 7, 76131 Karlsruhe, Germany

**Abstract** In order to enable high quality recycling of polypropylene (PP) plastic, additional classification and separation into the degree of degradation is necessary. In this study, different PP plastic samples were produced and degraded by multiple extrusion and thermal treatment. Using near infrared spectroscopy, the samples were examined and regression models were trained to predict the degree of aging. The models of the multiple extruded samples showed high accuracy, despite only minor spectral changes. The accuracy of the models of the thermally aged samples varied with the design of the training set due to the non-linear aging process, but showed sufficient accuracy in prediction.

**Keywords** Hyperspectral imaging, Plastic waste, Multiple Extrusion, Thermal aging, Regression, Sensor-based sorting

## 1 Introduction

With their versatile applications, plastics are indispensable for a high living standard in all areas of life, be it hygiene, lightweight construction and transport, food supply or technology [1, 2]. The plastic production worldwide amounts to 390 mio. t (2021) and in Germany alone, around 12 mio. t are consumed every year [3]. This causes massive

plastic waste streams, which are currently mainly disposed of through energy recovery in Europe and by landfill in most other regions of the world [4, 5]. However, so-called *end-of-life*-plastics are an important resource both for the plastic industry through mechanical recycling and the chemical industry through chemical recycling, yielding recycled plastic materials and platform chemicals and monomers respectively [6,7]. To underline their economical and environmental potential, plastic waste streams are referred to as *secondary raw materials* [8]. Special focus needs to be laid on the recycling of *post-consumer* secondary raw materials, which are plastics which have undergone their service-life once, as opposed to *pre-consumer*- or *post-industrial* materials, as the recycling rates of the former are very low [3,4,9].

For plastics recycling, particularly mechanical recycling, the quality of the resulting recyclate strongly depends on the characteristics of the input stream. The material homogeneity is therefore an important prerequisite for the input stream. To achieve this, the input stream is pre-processed and sorted in multiple stages, where sensor-based sorting plays a crucial role. The umbrella term *sensor-based sorting* describes a family of systems that enable the physical separation of individual particles from a material stream on the basis of information acquired by one or multiple sensors. A particular strength of the technology is its flexibility in terms of the criteria according to which sorting can be performed. This flexibility exists due to the variety of eligible sensor principles as well as the freely programmable data evaluation.

## 1.1 Contribution

During their service life, plastics undergo an aging process, inducing changes in the material's chemical and physical properties and potentially compromising its quality [10]. There are multiple factors which cause degradation effects during processing and service life such as thermo-mechanical stress during processing, causing chain scission and/or cross linking, exposure to UV-radiation, humidity, high temperatures or other weathering conditions, causing (thermo-)oxidative degradation [8, 11]. The mechanism of the oxidative degradation of polymers is referred to as autoxidation [12]. In the case of polypropylene (PP), autoxidation occurs after an induction period, accelerating the degradation exponentially [13]. Metal impurities from catalyst

residues may accelerate this process still further [14]. To counteract material degradation and to compensate a negative influence by aged polymers, stabilizers, compatibilizers and other additives are used [15]. Detailed knowledge of the degree of degradation of a secondary raw material stream is therefore highly useful for determining and adjusting the composition and concentration of the master batch in question, thereby improving the recycling of mixed materials with varying degrees of degradation.

In this study, a virgin PP homo-polymer has undergone two separate accelerated aging experiments. The first has been a recycling simulation by multiple processing and the second a service life simulation using an oven and thermo-oxidative conditions. The test specimen were injection-moulded and analyzed using NIR spectroscopy. Regression models were trained using NIR spectra to model the aging stage and predict the degree of degradation of unknown samples.

## 1.2 Related Work

Existing work has demonstrated the general suitability of NIR spectroscopy for age prediction of plastic samples. In [16], different types of plastics (virgin polymers) were investigated and regression models were trained using NIR spectra to predict the polymer degradation and a polymer quality assessment of the samples, caused by controlled, laboratory thermal aging. It showed the general suitability of NIR spectroscopy for determining polymer degradation, however accuracy depends on the type of plastic. Acrylonitrile butadiene styrene (ABS) and polyethylene terephthalate (PET) proved to be particularly suitable, while low-density polyethylene (LDPE) and PP were more difficult to evaluate. The chemical stability of polyethylene (PE) and PP was named as the cause. In [17], the investigations were extended to include the prediction of the extrusion cycles, which also showed differences in accuracy depending on the type of plastic. It was recommended to include more data in the model generation. Specifically, the prediction of the age of thermally treated PP samples was the subject of [18], with focus on the chemical modification of the polymer structure. In [19], the investigations were extended to plastic waste degraded under natural circumstances.

## 2 Materials and Methods

In the following, the production of the PP plastic samples is outlined. Subsequently, the data acquisition and the calculation of the regression models for the prediction of the aging stage are described.

### 2.1 Accelerated aging of test specimen

A PP homo-polymer (Moplen HP 500N, LyondellBasell, Rotterdam, Netherlands) in granular form was used as raw material for the accelerated aging experiments. Multiple processing was performed using a twin-screw extruder (Thermo Scientific™HAAKE™Rheomex PTW 16, Thermo Fisher, Waltham, Massachusetts, US) with a processing temperature range of 185 - 236 °C and 200 rpm. The extrusion process was repeated five times. From each extrusion cycle, a quantity was used for the preparation of test specimen (plates, 80 x 80 x 2.5 mm). Test specimen for further analysis were produced using an injection moulding system (Allrounder 320 C, Arburg, Loßburg, Germany). For the thermo-oxidative aging, test specimen were injection moulded immediately from the raw material using the above mentioned injection moulding system and conditions. The plates were placed in an aging furnace (Mettmert Universalschrank UF75, Mettmert, Büchenbach, Germany) at 150 °C and 100% ventilation. An overview can be found in Table 1.

**Table 1:** Overview of the two datasets consisting of differently aged PP samples.

	Dataset A	Dataset B
Plastic type	PP	PP
Material	Moplen HP 500N	Moplen HP 500N
Treatment	extrusion	thermal
Aging state parameter	1, 3, 5 (times)	10, 22, 27, 30, 34 (days)
Number of samples	3x10	5x10

### 2.2 Data acquisition

Due to the possibility to distinguish different types of plastics, the use of hyperspectral cameras in the near-infrared (NIR) wavelength range

is widespread within the sensor-based sorting industry [20]. Based on the chemical molecules present, or specifically their functional groups, different types of plastics have individual absorption characteristics and therefore show distinct spectra in the NIR wavelength range. On an experimental level, the sensor technology has also been used to investigate different characteristics, e. g., aging states of plastic. However, the use of NIR spectra for plastic age prediction is limited due to several possible properties. Regression on the basis of NIR spectra is an inverse problem, i. e., the exact composition of the sample cannot be derived from the spectral information. One problem is the overlap of the absorption bands [21,22].

For this study, the specimen were recorded using a hyperspectral NIR line-scan camera in the wavelength range of 900 – 1700 nm. The camera model is FX17 from Specim, consisting of a spatial resolution of 640 pixels. Per pixel, 256 spectral bands were acquired, resulting in a spectral resolution of slightly more than 3 nm. Due to different reflection properties caused by surface characteristics and camera position, variations occur in the raw spectra falling through the camera apparatus and captured by the sensor. These so-called scatter effects are minimized with the help of pre-processing steps.

First, the output of the hyperspectral sensor, which can be interpreted as the spectral reflectance, was converted to absorption units  $a = \log(1/R)$ . The wavelength range was then cropped to avoid unwanted edge effects. To minimize scattering effects, the Signal Normal Variant (SNV) was applied. The mean value of each spectrum is subtracted and then divided by its standard deviation.

### 2.3 Evaluation of the NIR spectra of aged PP samples

For each image, the foreground pixels were segmented and an average absorption spectrum was calculated from all spectra within the sample mask. This turned out to be a relevant measure to suppress noise effects and to better highlight the small spectral changes. The mean NIR absorption spectra within a degradation stage are shown in Figure 1. Clearly visible absorption bands of the NIR spectrum are associated with  $CH_2$  and  $CH_3$  groups of the PP molecules. In the range between 1100 and 1225 nm as well as 1350 to 1450 nm, absorption bands of the second overtone region of the methylene and methyl group or the

respective combination vibrations with  $CH$  groups are located. Absorption bands of the  $CH_3$  groups are located at lower wavelengths (1195 nm, 1360 nm) compared with  $CH_2$  absorption bands (1215 nm, 1395 nm) [23]. Due to the spectral proximity, there is a strong overlap of the absorption bands.

When looking at the samples that have been extruded several times, a decrease in the intensity of the absorption bands associated with  $CH_2$  and  $CH_3$  can be observed. A linear relationship between spectral changes and the number of extrusion cycles can be assumed. The observations can be explained by the increasing degradation of the polymer chains per extrusion cycle.

The observation of the spectra of the thermally aged PP samples show a similar course, but clear differences are recognizable. The thermally aged samples clearly show inhomogeneous degradation behavior related to the spatial area, visible as spots on the surface. The extracted local NIR spectra of a sample therefore show different aging stages depending on the spatial pixel position. With increasing thermal age, the intensity of the  $CH_3$  and  $CH_2$  absorption bands decreases. The behavior is clearly non-linear and can rather be modeled as an exponential relationship. Furthermore, stabilizing additives prevent chain scission at the beginning of aging. Once the additives are consumed, the aging process takes its exponential course. The start of the exponential aging process therefore has an induction period.

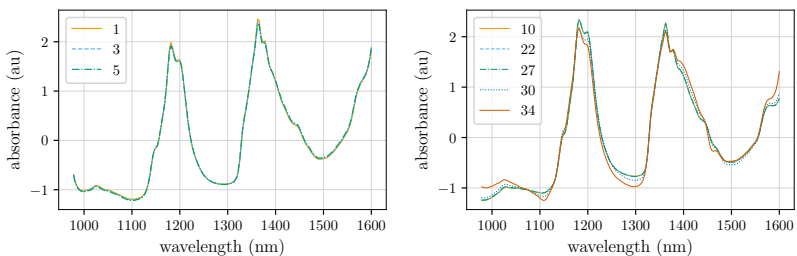


**Figure 1:** Mean absorption spectra of multiple extruded PP samples (1-, 3- and 5-fold extruded) after SNV (left) and mean absorption spectra of thermally aged PP samples (10, 22, 27, 30, 34 days) after SNV (right).

## 2.4 Regression-based age prediction

Linear regression models were trained to predict the degree of degradation of the PP samples based on the NIR absorption spectra. For this purpose, Partial Least Squares (PLS) Regression was used. The algorithm is based on the assumption of a linear relationship  $y = Xb$  between the input data  $X$  (spectral data) and the target values  $y$  (aging time or extrusion cycles). Even though this is not the case, especially for the thermally aged samples, its application in hyperspectral data evaluation has nevertheless proved successful and showed good results even for non-linear datasets [24]. The algorithm projects the data into a space with a smaller dimension, depending on the number of latent variables (LV) defined manually beforehand. The ability to model complex relationships increases with the number of LVs, but runs the risk of overfitting. The selection of the parameter is therefore crucial. When calculating the regression model, the number of LVs must be specified. This largely determines the ability of the model to adapt to complex data. In order to obtain a highly generalizing model using only a small amount of training data, a trade-off in the training stage is necessary. To determine the number, Leave-One-Out Cross-Validation was used. In each run, one partition is used as the test set and one model is trained with the remaining partitions. A metric is calculated for each model and then averaged over the metric values to obtain an overall assessment of the suitability of the parameterization of the model. This is done for a given number of LVs, and then the number of the best, most generalized model is chosen.

### Extrusion cycle prediction model

To calculate the PLS regression for Dataset A, 10 single-extruded and 10 five-extruded samples were used for training. The remaining 10 triple-extruded samples formed the independent test set. The optimization of the numbers of LVs resulted in a number of 5, this value was later used for calculation of the PLS model.

### Thermal age prediction model

The investigations were divided into two parts, both using Dataset B. First, it was analyzed whether linear regression is suitable to model the nonlinear aging process by using only a few target values. For this purpose, the samples with aging stages 10, 27 and 34 (days) were used for training. The calculated model (Model 1) was evaluated using test data obtained from the samples with aging stages 22 and 30 (days). For the model calculation, a LV number of 8 was used after optimization.

In a second study, all 5 aging stages were used for model training. For this purpose, 5 samples per aging stage were selected for model training and 5 samples each were used for the test set. Thus, the total number of spectra used for model training was reduced compared to the first study, but included a wider range of target values. The model (Model 2) was calculated using a number of 8 LVs.

### Evaluation metrics

As a metric to evaluate the regression model, the Root Means Squared Error (RMSE) and  $R^2$  score is used. The RMSE score

$$\text{RMSE} = \sqrt{\frac{\sum_{i=1}^n (\hat{y}_i - y_i)^2}{n}} \quad (1)$$

estimates the standard deviation of the prediction of a regression model. Here,  $\hat{y}_i$  describes the prediction result and  $y_i$  the ground truth value. A distinction can be made between the RMSE of the calibration set (training) and the prediction set (test). In addition, the  $R^2$  score

$$R^2 = 1 - \frac{\sum_{i=1}^n (y_i - \hat{y}_i)^2}{\sum_{i=1}^n (y_i - \bar{y})^2} \quad (2)$$

indicates how well the independent variables are suited to explain the variance of the dependent variables, where  $n$  is the number of samples.

## 3 Experimental Results

The performance of the regression models for predicting the age of PP plastics is examined below. A distinction is made between thermal aging and aging by multiple extrusion.



### 3.1 Extrusion cycle prediction results

The performance of the model was analyzed by calculating the RMSE and  $R^2$  of the test set. Both values are depicted together with the exact structure of the training and test set in Table 2. The model achieved an RMSE of 0.367 on the independent test data of the aging stage not yet considered during training. Figure 2 shows the model-predicted values plotted against the real values. The results show a general suitability of the model for the estimation of extrusion cycles. The calculated RMSE of the training data of 0.118 shows similarity to the obtained value in the test data. In addition, the calculation of the median of the estimated aging states of the test data ( $\tilde{y}_{pred} = 3.052$ ) shows that the results scatter around the target value. The data show a linear correlation between the target value and the spectral information. Therefore, the linear PLS model can model the correlation with high accuracy using only two aging stages during training. During model calculation, it has been shown that the main focus must be on the generation of the training data and its pre-processing. Only the calculation of mean value spectra makes it possible to visualize the small change in the absorption spectrum with respect to noise influences. Thus, multiple extrusion leads only to a small change in the functional groups.

**Table 2:** Performance of the regression models on a respective independent test set for the prediction of the thermal aging stage resp. the number of extrusion cycles.

	Train	Test A	LV	RMSE	$R^2$
Dataset A	1, 5	3	5	0.367	-
Dataset B, Model 1	10, 27, 34	22, 30	8	2.158	0.709
Dataset B, Model 2	10, 22, 27, 30, 34	10, 22, 27, 30, 34	8	1.437	0.970

### 3.2 Thermal age prediction results

The age-prediction models of PP were assessed by calculating the RMSE and  $R^2$  of the test set. Both values are depicted together with the exact structure of the training and test set in Table 2. Figure 4 shows the model-predicted values plotted against the real values.

The evaluation of the thermally aged PP samples resulted in the calculation of two models, each based on different training data or

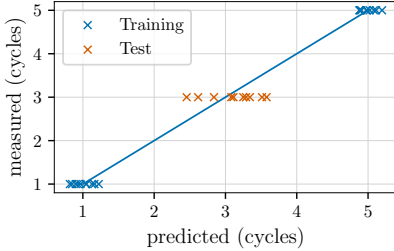


**Figure 2:** Results of the regression model for predicting the number of extrusion cycles. Measured versus predicted number of cycles.

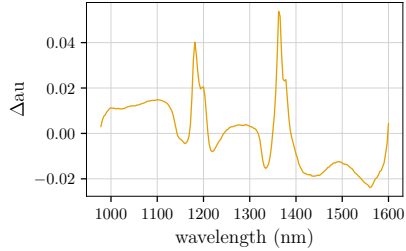


**Figure 3:** Difference of the mean NIR absorption spectra of all 1-fold and the 5-fold extruded PP samples used for model training.

different aging stages. The analysis of the spectra already showed a nonlinear course of aging. The first model, calculated from only three aging stages, achieved an RMSE of 2.158 on the test data. The scatter of the estimated aging highlights the problem of modeling the nonlinear aging process using a few target values. Prediction of the 22 days aged samples was consistently overestimated, illustrated by the median  $\tilde{y}_{pred,22} = 23.292$ . In contrast, the 30 days aged samples were only slightly overestimated on average ( $\tilde{y}_{pred,30} = 31.367$ ), but the values strongly scatter ( $\sigma_{y_{pred,30}} = 2.324$ ). The RMSE of the training data of 0.696 is also significantly lower than the RMSE of the independent test data. In addition to the nonlinear aging process, the tests also confirmed a delayed start of the aging process by admixed additives.

For the second regression model, the training set was adapted by including all 5 aging stages. The test set resulted in an RMSE of 1.437. The RMSE of the training data of 0.857 is similarly low. In addition, comparison of the medians of the test and training sets shows a uniform spread of the estimated target values around the real ones.

The comparison of both models showed that more aging stages in the training set are more important to model the nonlinear course than the absolute number of training spectra. Furthermore, it was shown that despite local differences in the aging stages within a sample, the mean spectra is suitable to represent the aging time of the entire sample.

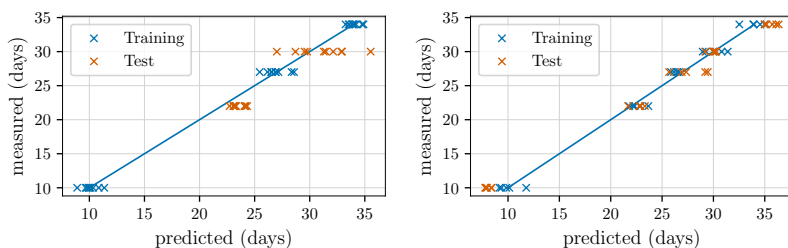


**Figure 4:** Results of the regression models of thermally aged PP samples, measured versus predicted days. Model 1 (left) and Model 2 (right).

## 4 Conclusion and Future Work

The investigations showed the general suitability of NIR spectroscopy for the prediction of different aging and degradation stages of PP plastic. Thermally aged as well as multiple extruded PP samples were investigated. Different regression models were calculated to estimate the duration of thermal aging or the number of extrusion passes. Special attention was paid to the pre-processing and spectral averaging of the NIR spectra in order to make small spectral differences visible. The calculated regression models showed a correlation between aging condition and spectral information. The exponential progression of thermally aged samples must be modeled sufficiently well. More target values in model training greatly improves the generalizability of the model. One challenge is the inhomogeneous aging visible on the spatial area of the samples and therefore impacting the spectra, which can be investigated in further studies.

## Acknowledgment

This work was supported as a Fraunhofer LIGHTHOUSE PROJECT.

## References

1. R. Mülhaupt, "Green polymer chemistry and bio-based plastics: dreams and reality," *Macromolecular Chemistry and Physics*, vol. 214, no. 2, pp. 159–

174, 2013.

2. C. G. Schirmeister and R. Mülhaupt, "Closing the carbon loop in the circular plastics economy," *Macromolecular Rapid Communications*, vol. 43, no. 13, p. 2200247, 2022.
3. P. Europe, "Plastics - the facts 2022," <https://plasticseurope.org/knowledge-hub/plastics-the-facts-2022/>, 2022.
4. R. Geyer, J. R. Jambeck, and K. L. Law, "Production, use, and fate of all plastics ever made," *Science advances*, vol. 3, no. 7, p. e1700782, 2017.
5. R. Meys, F. Frick, S. Westhues, A. Sternberg, J. Klankermayer, and A. Bardow, "Towards a circular economy for plastic packaging wastes—the environmental potential of chemical recycling," *Resources, Conservation and Recycling*, vol. 162, p. 105010, 2020.
6. S. Al-Salem, P. Lettieri, and J. Baeyens, "Recycling and recovery routes of plastic solid waste (psw): A review," *Waste management*, vol. 29, no. 10, pp. 2625–2643, 2009.
7. S. Yin, R. Tuladhar, F. Shi, R. A. Shanks, M. Combe, and T. Collister, "Mechanical reprocessing of polyolefin waste: A review," *Polymer Engineering & Science*, vol. 55, no. 12, pp. 2899–2909, 2015.
8. F. Vilaplana and S. Karlsson, "Quality concepts for the improved use of recycled polymeric materials: a review," *Macromolecular Materials and Engineering*, vol. 293, no. 4, pp. 274–297, 2008.
9. M. K. Eriksen, A. Damgaard, A. Boldrin, and T. F. Astrup, "Quality assessment and circularity potential of recovery systems for household plastic waste," *Journal of Industrial Ecology*, vol. 23, no. 1, pp. 156–168, 2019.
10. A. Jansson, K. Möller, and T. Gevert, "Degradation of post-consumer polypropylene materials exposed to simulated recycling—mechanical properties," *Polymer Degradation and Stability*, vol. 82, no. 1, pp. 37–46, 2003.
11. E. Strömberg and S. Karlsson, "The design of a test protocol to model the degradation of polyolefins during recycling and service life," *Journal of Applied Polymer Science*, vol. 112, no. 3, pp. 1835–1844, 2009.
12. L. M. Smith, H. M. Aitken, and M. L. Coote, "The fate of the peroxy radical in autoxidation: how does polymer degradation really occur?" *Accounts of chemical research*, vol. 51, no. 9, pp. 2006–2013, 2018.
13. A. Jansson, K. Möller, and T. Hjertberg, "Chemical degradation of a polypropylene material exposed to simulated recycling," *Polymer degradation and stability*, vol. 84, no. 2, pp. 227–232, 2004.

14. G. W. Ehrenstein and S. Pongratz, *Beständigkeit von Kunststoffen*. Hanser München, 2007.
15. R. Pfaendner, H. Herbst, K. Hoffmann, and F. Sitek, "Recycling and restabilization of polymers for high quality applications. an overview," *Die Angewandte Makromolekulare Chemie: Applied Macromolecular Chemistry and Physics*, vol. 232, no. 1, pp. 193–227, 1995.
16. A. Alassali, S. Fiore, and K. Kuchta, "Assessment of plastic waste materials degradation through near infrared spectroscopy," *Waste management*, vol. 82, pp. 71–81, 2018.
17. A. Alassali, C. Picuno, T. Bébien, S. Fiore, and K. Kuchta, "Validation of near infrared spectroscopy as an age-prediction method for plastics," *Resources, Conservation and Recycling*, vol. 154, p. 104555, Mar. 2020.
18. H. Shinzawa, R. Watanabe, S. Yamane, M. Koga, H. Hagihara, and J. Mizukado, "Aging of polypropylene probed by near infrared spectroscopy," vol. 29, no. 5, pp. 259–268.
19. X. Chen, N. Kroell, T. Dietl, A. Feil, and K. Greiff, "Influence of long-term natural degradation processes on near-infrared spectra and sorting of post-consumer plastics," *Waste Management*, vol. 136, pp. 213–218, 2021.
20. D. J. da Silva and H. Wiebeck, "Current options for characterizing, sorting, and recycling polymeric waste," *Progress in Rubber, Plastics and Recycling Technology*, vol. 36, no. 4, pp. 284–303, 2020.
21. M. Vidal, A. Gowen, and J. M. Amigo, "Nir hyperspectral imaging for plastics classification," *NIR news*, vol. 23, no. 1, pp. 13–15, 2012.
22. Q. Duan and J. Li, "Classification of common household plastic wastes combining multiple methods based on near-infrared spectroscopy," *ACS ES&T Engineering*, vol. 1, no. 7, pp. 1065–1073, 2021.
23. J. Gulmine, P. Janissek, H. Heise, and L. Akcelrud, "Polyethylene characterization by ftir," *Polymer testing*, vol. 21, no. 5, pp. 557–563, 2002.
24. M. Blanco, J. Coello, H. Iturriaga, S. MasPOCH, and J. Pages, "Nir calibration in non-linear systems: different pls approaches and artificial neural networks," *Chemometrics and Intelligent Laboratory Systems*, vol. 50, no. 1, pp. 75–82, 2000.